




Smart pH-responsive nanoparticles in a model tumor microenvironment for enhanced cellular uptake

Jie Pan^{1,*} , Shuaiquan Lei¹, Lu Chang¹, and Dong Wan^{1,*}

¹ School of Environmental and Chemical Engineering, Tianjin Polytechnic University, Tianjin 300387, China

Received: 9 July 2018

Accepted: 14 September 2018

Published online:

20 September 2018

© Springer Science+Business Media, LLC, part of Springer Nature 2018

ABSTRACT

In this study, novel smart pH-sensitive nanoparticles of PLA-mPEG₂₀₀₀/TPGS₃₃₅₀-PHis-Folate for enhanced effect of chemotherapy are developed. Polyethylene glycol (PEG) is decorated on the surface of nanocarriers in order to prolong the circulation of nanoparticles in blood; the pH-sensitive material of poly(L-histidine) is utilized in nanoparticles for the intelligent purposes: under normal physiological pH, the targeting molecule of folate can be hidden into the layer of PEG in nanoparticles, which closes the active targeting function of nanoparticles; but in weak acid of tumor tissue, poly(L-histidine) is protonated to expose folate on the surface of nanoparticles, opening the active targeting function; next, nanoparticles are internalized by cells via folate receptor-mediated endocytosis; finally, poly(L-histidine) in endosome/lysosome begins to dissociate, leading to quick intracellular drug release. The features of the nanoparticles such as morphology, particle size, drug loading content, in vitro release and in vitro cytotoxicity are further investigated. Nanoparticles designed in this work have multiple functions such as active targeting, long circulation and easy internalization by cells simultaneously, and rapid intracellular drug release, which demonstrates huge potential to apply for the efficient treatment of cancer.

Introduction

Cancer is a major public health problem in the world [1]. Chemotherapy as a usual approach applies chemical drugs for controlling the proliferation, infiltration and metastasis of cancer cells [2, 3]. Compared with traditional therapeutic formulations, drug-loaded nanocarriers such as liposomes, micelles, polymeric and drug conjugates offer various advantages including enhanced efficiency of drug

delivery, reduced systemic side effects of drug, protection of a drug before entering into cancer cells, and so on, resulting in improved therapeutic efficacy for cancer [4, 5].

It was reported in 2015 that although drug-loaded nanocarriers offer many attractive features in the treatment of cancer, nanocarriers face several biological barriers in drug delivery such as opsonization and subsequent sequestration by the mononuclear phagocyte system (MPS), nonspecific distribution,

Address correspondence to E-mail: panjie@tjpu.edu.cn; wandong_tjpu@126.com

cellular internalization, escape from endosomal, and so on, which significantly decrease drug's therapeutic efficacy [6, 7]. Therefore, the ideal nanocarriers should have these characteristics: (1) long circulation time in blood; (2) enrichment in tumor tissue; (3) to facilitate tumor cell uptake; (4) fast and effective intracellular drug release [8–11]. For example, researchers generally exploited polyethylene glycol (PEG) or PEG-based material for surface modification of nanocarriers in order to extend circulation time in blood of the nanocarriers [12, 13]. But PEG modification can inhibit frequently endocytosis of nanocarriers by cells to reduce drug accumulation in cancer cells, resulting in reduced chemotherapy efficacy [14].

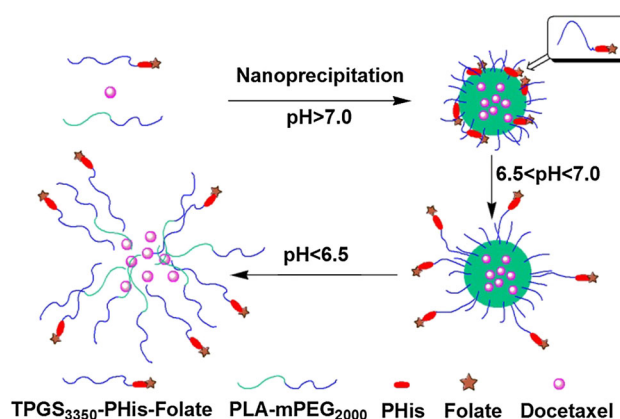
In the recent decades, in order to overcome biological barriers of nanocarriers encountered in drug delivery, stimulus-sensitive nanocarriers were developed to trigger drug release in response to specific external stimuli (such as light, ultrasound, electric field, magnetic field and heating) or internal stimuli (such as variation in pH value or concentrations of ions, small molecules and enzymes) [15–17]. For example, many pH-sensitive nanocarriers were fabricated to enhance anticancer efficacy of drug through exploiting intrinsic differences in pH values between normal tissues (pH 7.4) and extracellular environment of solid tumors (pH 6.5–6.8) [18–22]. Moreover, after entering into cancer cells via endocytosis pathway, nanocarriers often face early endosomes (pH 5.5–6.0) and lysosomes (pH 5.0–5.5), which could be helpful for fast intracellular drug release [23, 24].

The imidazole ring in poly(L-histidine) (PHis) has an electron lone pair on the unsaturated nitrogen, resulting in the pH-sensitive property of PHis. Moreover, PHis-based nanocarriers achieved endosomal escape in acidic subcellular compartments such as endosomes through proton sponge effect. PHis-based nanocarriers have thus great potential as an acid triggering tumor-killing platform [25–28]. For example, Bae et al. described that pH-sensitive PHis-PEG/PLLA-PEG mixed micelles were developed for the treatment of cancer [25]. Furthermore, Lin Mei et al. synthesized pH-sensitive nanoparticles of poly(L-histidine)-poly(lactide-co-glycolide)-tocopheryl polyethylene glycol succinate (PHis-PLGA-TPGS) for antitumor drug delivery [26].

D- α -Tocopheryl polyethylene glycol succinate (TPGS) is a water-soluble derivative of natural

vitamin E, acting as an effective emulsifier because of its bulky structure and large surface area, resulting in higher emulsification effect, higher drug encapsulation efficiency [29]. TPGS₃₃₅₀ with PEG₃₃₅₀ groups are particularly effective steric stabilizers to shield nanoparticles from opsonization and phagocytosis, improving the aqueous solubility of nanoparticles [30, 31]. Our group also prepared TPGS₃₃₅₀-QDs nanoparticles for cellular imaging, and these nanoparticles demonstrated excellent colloidal stability and reduced nonspecific cellular uptake due to the effect of TPGS₃₃₅₀ [32].

In this work, pH-sensitive PLA-mPEG₂₀₀₀/TPGS₃₃₅₀-PHis-Folate nanoparticles were fabricated through nanoprecipitation method, and docetaxel was used as a model anticancer drug. The scheme of drug-loaded smart pH-sensitive nanoparticles and their structural changes under different pH values is presented in Scheme 1. It was hypothesized in this work that targeting molecules of folate were hidden by the PEG₂₀₀₀ chains in PLA-mPEG₂₀₀₀ at normal pH, while PHis in TPGS₃₃₅₀-PHis-Folate was protonated under lowered pH of tumor tissue to enable PEG₃₃₅₀ chains in TPGS₃₃₅₀ stretch out of nanoparticles' surface, resulting in exposing folate on the outermost surface of nanoparticles. After internalized via the folate receptor-mediated endocytosis pathway, these nanoparticles quickly released drug in the inner of cells under the effect of acid conditions in endosome/lysosome. Nanoparticles developed in this study illustrated multiple functions including active targeting, long circulation and easy cellular uptake simultaneously, and rapid intracellular drug release,



Scheme 1 The schematic of drug-loaded smart pH-sensitive PLA-mPEG₂₀₀₀/TPGS₃₃₅₀-PHis-Folate nanoparticles and their structural changes under different pH values.

which significantly improve the anticancer effects of chemotherapy and reduce toxic side effects of drug.

Materials and methods

Materials

Docetaxel (anhydrous, 99.8%) was purchased from Shanghai Jinhe Bio-Pharmaceuticals Co. Ltd, China. N^{α} -CBZ- N^{im} -DNP-L-histidine was obtained from GL Biochem. Co. Ltd. (Shanghai, China). D - α -Tocopheryl succinate, polyoxyethylene bis (amine) (MW 3350) were purchased from Aladdin Industrial Corporation (Shanghai, China). Dichloromethane (DCM) and Tween 80 were purchased from Tianjin Kemiou Chemical Reagent Co. Ltd. D - α -Tocopheryl polyethylene glycol succinate (TPGS), Folic acid, N,N' -dicyclohexylcarbodiimide (DCC), N -hydroxysuccinimide (NHS), triethylamine (TEA), dimethyl sulfoxide (DMSO), trypsin-EDTA solution were all purchased from Sigma-Aldrich (St. Louise, MO, USA). PLA₁₆₀₀₀-mPEG₂₀₀₀ was purchased from Shandong Institute of Medical Instruments, China. Coumarin-6 was obtained from J&K Scientific Ltd. (Beijing, China). Dimethylformamide (DMF), anhydrous diethyl ether, 2-mercaptoethanol were purchased from Bodi Drug Manufacturing Co. Ltd. (Tianjin, China). Cell counting kit-8 assay (CCK-8) was obtained from Beyotime Institute of Biotechnology, China.

Synthesis of poly(N^{im} -DNP-L-histidine), TPGS₃₃₅₀-NH₂, TPGS₃₃₅₀-PHis

N^{α} -CBZ- N^{im} -DNP-L-histidine was transformed to the N^{im} -DNP-L-histidine (NCA) with thionyl chloride. Briefly, 2.4 mL thionyl chloride was added to the solution of 5 g N^{α} -CBZ- N^{im} -DNP-L-histidine dissolved in 30 mL anhydrous THF, agitating about 5 min to obtain a clear solution [33]. Next, excess cold diethyl ether was added to precipitate N^{im} -DNP-L-histidine carboxyanhydride. TPGS₃₃₅₀-NH₂ was synthesized by a procedure reported in a publication [30]. In a brief, D - α -Tocopheryl succinate, PEG₃₃₅₀ bis-amine, DCC and NHS (stoichiometric ratio of 1:1.2:2:2) were mixed to stir in a nitrogen environment at dark for 2 days. TPGS₃₃₅₀-NH₂ can be obtained through filtering, precipitated in cold diethyl ether and freeze drying. TPGS₃₃₅₀-NH₂ was

utilized to initiate the ring-opening polymerization NCA at room temperature in a nitrogen environment for 3 days [19, 33, 34]. Then TPGS₃₃₅₀-poly(L-histidine) (TPGS₃₃₅₀-PHis) with amino-terminated was formed and precipitated in cold diethyl ether and freeze drying.

Synthesis of TPGS₃₃₅₀-PHis-Folate and TPGS₃₃₅₀-Folate

TPGS₃₃₅₀-PHis-Folate was synthesized through coupling TPGS₃₃₅₀-PHis with folate via N -hydroxysuccinimide to yield triblock copolymer. In detail, 1 mmol TPGS₃₃₅₀-PHis in 30 mL dimethyl sulfoxide was coupled with 1 mmol folate at room temperature for 1 day, in the presence of 1.25 mmol DCC and 1.5 mmol NHS. The byproduct was filtered, and the filtrate was dialyzed with pre-swollen dialysis membrane tube (Spectra/Por; MWCO 3350) to remove unconjugated polymer. Next, 2-mercaptoethanol was added for deprotection of triblock copolymer followed by dialyzing against DMSO for 1 day and deionized water for 2 days. After freeze-dried, TPGS₃₃₅₀-PHis-Folate was obtained. TPGS₃₃₅₀-Folate was synthesized as follows: folate (1 mmol) was dissolved in DMSO (30 mL) and stirred with DCC (1.2 mmol) and NHS (2 mmol) at 50 °C for 6 h. After filtration to remove DCU, FOL-NHS was reacted with TPGS₃₃₅₀-NH₂ (stoichiometric molar ratio of 1:1) at room temperature overnight for 1 day. Next, The final product TPGS₃₃₅₀-Folate was precipitated in cold diethyl ether, then dialyzed against water and freeze-dried [30].

Formulation of docetaxel-loaded nanoparticles

The docetaxel-loaded nanoparticles were prepared by the nanoprecipitation method [35]. 100 mg mixture of PLA-mPEG₂₀₀₀ and TPGS₃₃₅₀-PHis-Folate (2:1; 5:1; 10:1, weight ratios) and 10 mg docetaxel were dissolved in 8 mL DMSO. Next, the above solution was dropped into 120 mL of aqueous solution with 0.03% (w/v) TPGS as emulsifier and then dialyzed against water for 24 h to remove DMSO. After washed and centrifuged at 10000 rpm for 15 min, final nanoparticles were obtained. The docetaxel-loaded PLA-mPEG₂₀₀₀ and PLA-mPEG₂₀₀₀/TPGS₃₃₅₀-Folate nanoparticles were prepared using the same procedure.

Acid–base titration of PLA-mPEG₂₀₀₀/TPGS₃₃₅₀-PHis-Folate nanoparticles

PLA-mPEG₂₀₀₀/TPGS₃₃₅₀-PHis-Folate nanoparticles (weight ratio 5:1) were used to investigate pH sensitivity. The PLA-mPEG₂₀₀₀/TPGS₃₃₅₀-PHis-Folate nanoparticles (20 mg) were dispersed in 20 mL of deionized water, and pH of the nanoparticles solution was adjusted to pH 11 using 1 M NaOH. Next, 0.01 M HCl solution was added stepwise above nanoparticles solution to obtain the titration profile.

Determination of drug loading content and drug encapsulation efficiency

The drug loading content and encapsulation efficiency of nanoparticles were determined with HPLC (Agilent LC1100). In brief, 5 mg dry nanoparticles were dissolved with DCM, followed by evaporating overnight. Furthermore, 2 mL mobile phase (50:50 v/v acetonitrile/water) was added to extract. Next, the solution was filtered with a 0.22- μ m poly(vinylidene fluoride) (PVDF) syringe filter for HPLC analysis. The column was eluted with acetonitrile/water (50:50, v/v) at a flow rate of 1.0 mL/min. The column effluent was detected at 230 nm with a UV-Vis detector. Drug loading content and encapsulation efficiency were calculated as follows, respectively:

$$\text{DLC (\%)} = \frac{\text{Weight of drug in the nanoparticles}}{\text{Weight of drug loaded nanoparticles}} \times 100\%$$

$$\text{DEE (\%)} = \frac{\text{Weight of drug encapsulation in nanoparticles}}{\text{Amount of drug in the fabrication of nanoparticles}} \times 100\%$$

In vitro drug release at different pH values

Ten milligram of nanoparticles dispersed in 5 mL PBS (pH 5.0, 6.5, 7.4) was placed into a dialysis bag (MWCO 3350) and dialyzed against 25 mL of PBS (pH 5.0, 6.5, 7.4) containing 0.1% w/v Tween 80 in an orbital water bath shaking (100 rpm) at 37 °C. At designed time intervals, 0.5 mL solution was taken out and replaced with an equal volume of fresh PBS medium. The solution was extracted with DCM and transferred in mobile phase. After the evaporation of DCM and filtration using a 0.22 μ m pore size filter,

the released docetaxel concentration was detected at 230 nm by HPLC.

Cell culture

Murine breast cancer 4T1 cell lines were purchased from cell culture center of Institute of Basic Medical Sciences, Chinese Academy of Medical Sciences (Beijing, China). 4T1 cells were grown in RPMI-1640 medium containing 10% fetal bovine serum (FBS) and 1% penicillin–streptomycin in a humidified incubator at 37 °C with 5% CO₂.

In vitro cellular uptake of nanoparticles

After 12 h incubation, the adherent 4T1 murine breast cancer cells were washed twice with PBS. The pH of the culture medium was adjusted with 0.1 M HCl to a desired pH (pH 7.4, 6.8 and 5.8). The coumarin-6-loaded nanoparticles were prepared in the same way as that of the docetaxel-loaded nanoparticles except coumarin-6 instead of docetaxel was encapsulated in the nanoparticles. The suspension of Coumarin-6 loaded nanoparticles in the different pH medium at nanoparticles concentration 0.1 mg/mL was added into the chamber. After 4-h incubation, the nanoparticles suspension was removed and the wells were washed three times with 50 mL of PBS. Moreover, cells were fixed with 75% ethanol for 15 min. Finally, the cell was washed with PBS and recorded with confocal laser scanning microscope (CLSM) (Zeiss LSM 410).

In vitro cytotoxicity

A cell counting kit-8 (CCK-8) assay was utilized to measure the cytotoxicity of the nanoparticles. Briefly, 4T1 murine breast cancer cells were incubated in 96-well plates (Corning Inc., NY, USA). The pH of the culture medium was adjusted with 0.1 M HCl to a desired pH (7.4, 6.8 and 5.8). The several formulations (PLA-mPEG₂₀₀₀ nanoparticles, PLA-mPEG₂₀₀₀/TPGS₃₃₅₀-Folate nanoparticles and PLA-mPEG₂₀₀₀/TPGS₃₃₅₀-PHis-Folate nanoparticles) containing three different docetaxel concentrations (1, 4 and 10 μ g/mL) were added to 96-well plates. In vitro cytotoxicity in medium with pH 7.4, 6.8 and 5.8 were used as control. After 8 h incubation, cells were washed twice with PBS. After 10 μ L of CCK-8 supplemented with 90 μ L culture medium added into each well for 2-h incubation, the absorbance of each well was measured by the microplate reader of absorbance–wavelength at

450 nm minus background at 620 nm. Cell viability was calculated as the percentage of the absorbance from the wells containing the cells incubated with the nanoparticles suspension over that of the cells only.

Results and discussion

Synthesis of TPGS₃₃₅₀-PHis-Folate

TPGS₃₃₅₀-PHis-Folate copolymer was synthesized by the ring-opening polymerization in the presence of NCA and TPGS₃₃₅₀-NH₂ (initiator), followed by reacting with folate. The protected TPGS₃₃₅₀-PHis-Folate was reacted with 2-mercaptoethanol in DMSO to remove benzyl groups of poly(N^{im}-DNP-L-histidine). The synthesis route of TPGS₃₃₅₀-PHis-Folate is illustrated in Fig. 1.

The actual number of L-histidine units in the polymer was 15 (calculated from ¹H-NMR spectra), which is basically consistent with the designed number. Figure 2 shows the structure of synthesized TPGS₃₃₅₀-PHis-Folate detected with ¹H-NMR in DMSO-d₆. It could be observed in Fig. 2 that the peak at 3.51 ppm was assigned to the CH₂ protons of PEG part of TPGS₃₃₅₀. The peaks in the aliphatic region (signals at 2.69 and 2.85 ppm; signals at 2.35–1.84 ppm; signal at 1.09 ppm; signal at 0.82 ppm) belonged to various moieties of vitamin E tails. The peak at 11.43 ppm and peak at 6.63 and 7.86 ppm were attributed to the –COOH protons and benzene group protons of folate segment, and the imidazole ring of poly(L-histidine) (3.05, 6.65, 7.63 and 8.13 ppm) was also confirmed in ¹H-NMR spectrum.

Based on the findings from gel permeation chromatography (GPC), it should be noticed that Mw and Mn of TPGS₃₃₅₀-PHis-Folate were 7484 and 6143, respectively, which was not consistent with the ¹H-NMR data. It was reported that the molecular size in solution is also influenced by the molecular architecture [36], so the molecular weights of the copolymers from ¹H-NMR were exploited in the current study.

The drug loading content and encapsulation efficiency of nanoparticles are important factors for drug delivery systems. The drug loading content in PLA-mPEG₂₀₀₀ nanoparticles, PLA-mPEG₂₀₀₀/TPGS₃₃₅₀-Folate nanoparticles, PLA-mPEG₂₀₀₀/TPGS₃₃₅₀-PHis-Folate nanoparticles were 5.5%, 5.3% and 5.2%,

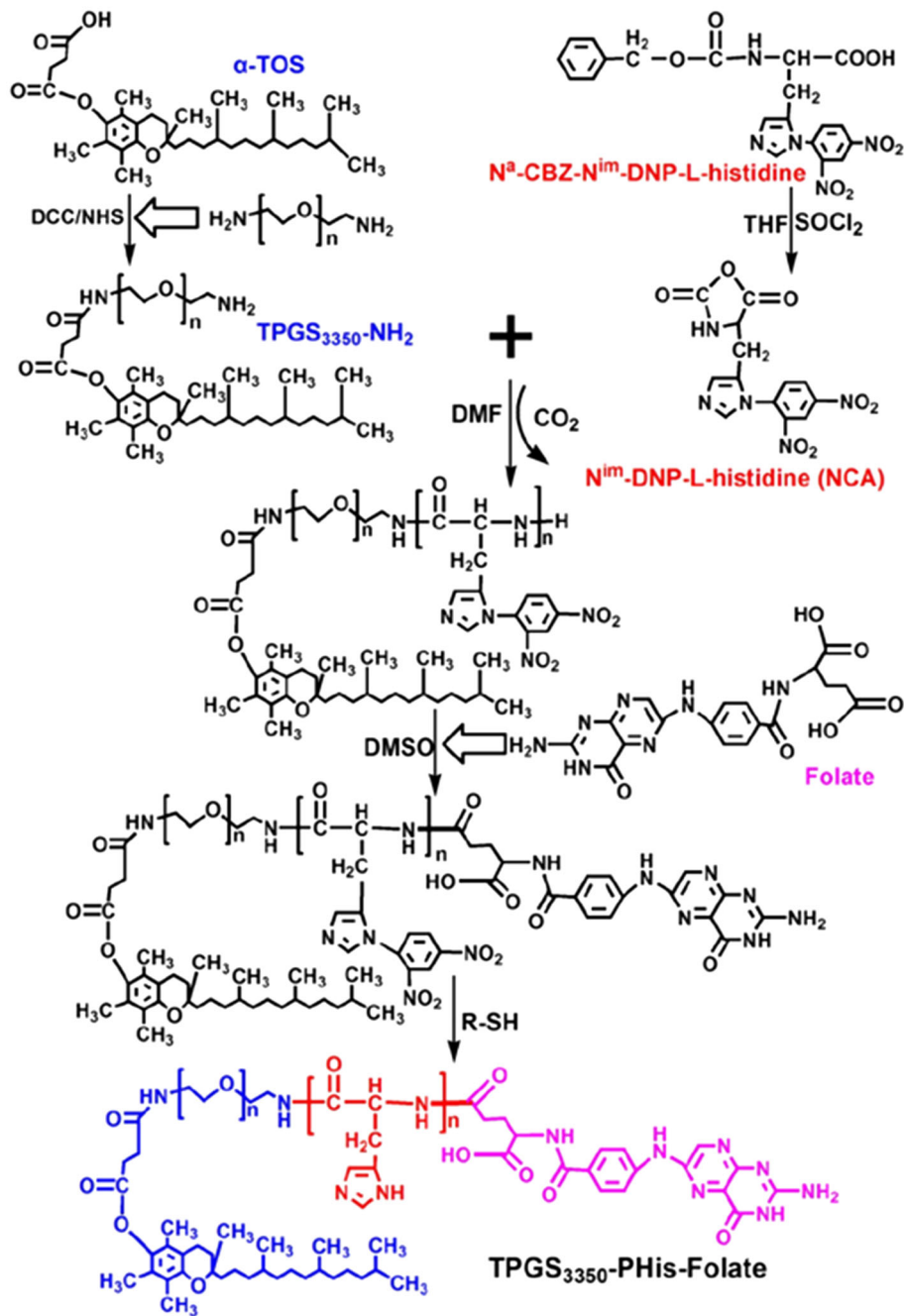
respectively. The drug encapsulation efficiency of PLA-mPEG₂₀₀₀ nanoparticles, PLA-mPEG₂₀₀₀/TPGS₃₃₅₀-Folate nanoparticles, PLA-mPEG₂₀₀₀/TPGS₃₃₅₀-PHis-Folate nanoparticles were found to be 60.3 ± 0.5%, 58.8 ± 0.7% and 57.7 ± 0.6%, respectively. These results present strong evidence that drug loading content and encapsulation efficiency of nanoparticles were not associated obviously with the amount of TPGS₃₃₅₀-PHis-Folate in nanoparticles.

Particle size, size distribution and zeta potential at different pH values

Herein, the change of size and zeta potential of nanoparticles at different pH values are key features, ensuring that the nanoparticles are smart nanoparticles for enhanced anticancer effect of chemotherapy. It can be seen from Fig. 3a that the particle sizes of the nanoparticles were varied as the pH change. There was no big difference in the particle size of PLA-mPEG₂₀₀₀ nanoparticles at pH from 8.0 to 5.0, which verified that the size and size distribution of PLA-mPEG₂₀₀₀ nanoparticles were not significantly affected by different pH values. But the mean diameter of the PLA-mPEG₂₀₀₀/TPGS₃₃₅₀-PHis-Folate nanoparticles was enlarged with decreasing pH value from 7.4 to 5.0 due to the protonation of poly(L-histidine). Consequently, the targeting molecule of folate in PLA-mPEG₂₀₀₀/TPGS₃₃₅₀-PHis-Folate nanoparticles could be buried in the hydrophilic PEG layer because of water insolubility of PHis at normal physiological pH 7.4, while folate was exposed on the outmost surface of nanoparticles due to water solubility of PHis at weak acid of tumor tissue (pH 6.8), which helped to carry out following folate receptor-mediated endocytosis.

The zeta potential of PLA-mPEG₂₀₀₀/TPGS₃₃₅₀-PHis-Folate nanoparticles at different pH values is shown in Fig. 3b. The PLA-mPEG₂₀₀₀ nanoparticles exhibited a stable zeta potential at pH from 5.0 to 8.0. But the zeta potential of the PLA-mPEG₂₀₀₀/TPGS₃₃₅₀-PHis-Folate nanoparticles was influenced by the weight ratio of the two polymer components. As shown in Fig. 3b, zeta potential of PLA-mPEG₂₀₀₀/TPGS₃₃₅₀-PHis-Folate nanoparticles was enhanced with decreasing pH due to the ionization of PHis segment. Furthermore, it can be found from Fig. 3b that PLA-mPEG₂₀₀₀/TPGS₃₃₅₀-PHis-Folate nanoparticles with high content of TPGS₃₃₅₀-PHis-Folate achieved slightly higher zeta potential than

Figure 1 The synthetic route of TPGS₃₃₅₀-PHis-Folate triblock copolymer.



those with low content of TPGS₃₃₅₀-PHis-Folate at same pH value. In this work, PLA-mPEG₂₀₀₀/TPGS₃₃₅₀-PHis-Folate (weight ratio 5:1) nanoparticles were selected for the further experiment.

Surface morphology

As shown in Fig. 4, PLA-mPEG₂₀₀₀/TPGS₃₃₅₀-PHis-Folate nanoparticles are about 250 nm in diameter with narrow size distribution. These nanoparticles

with smooth surface ensured them have long circulation time in blood compared to those with a rougher surface [37]. Moreover, the particle size detected with FESEM was good agreement with that determined by the laser light scattering.

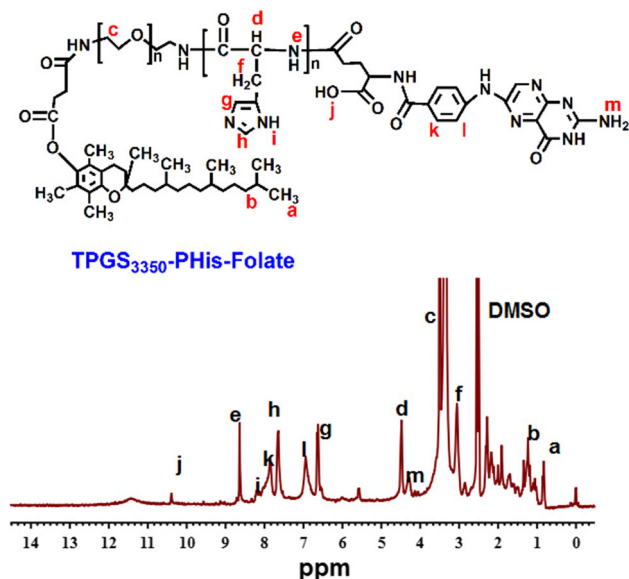


Figure 2 The ^1H NMR spectra of TPGS₃₃₅₀-PHis-Folate.

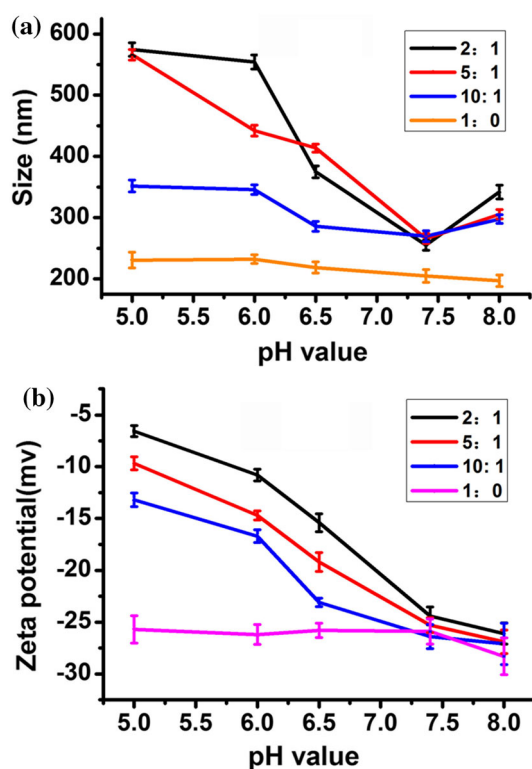


Figure 3 **a** Particle size of PLA-mPEG₂₀₀₀/TPGS₃₃₅₀-PHis-Folate nanoparticles with weight ratios of 1:0, 10:1, 5:1, 2:1 at different pH values; **b** zeta potential of PLA-mPEG₂₀₀₀/TPGS₃₃₅₀-PHis-Folate nanoparticles with weight ratios of 1:0, 10:1, 5:1, 2:1 at different pH values.

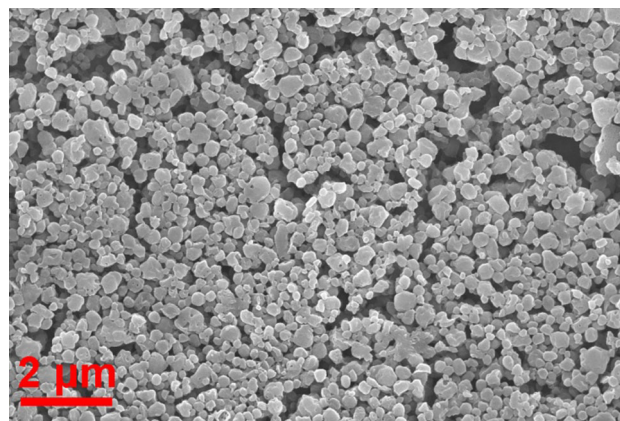


Figure 4 FESEM image of PLA-mPEG₂₀₀₀/TPGS₃₃₅₀-PHis-Folate nanoparticles with a weight ratio of 5:1.

Acid–base titration of PLA-mPEG₂₀₀₀/TPGS₃₃₅₀-PHis-Folate nanoparticles

The acid–base titration profile of PLA-mPEG₂₀₀₀/TPGS₃₃₅₀-PHis-Folate nanoparticles is shown in Fig. 5, indicating that the PLA-mPEG₂₀₀₀/TPGS₃₃₅₀-PHis-Folate nanoparticles were pH-sensitive. And the apparent pK_a of PLA-mPEG₂₀₀₀/TPGS₃₃₅₀-PHis-Folate nanoparticles was calculated as 6.42 based on the first-order derivation of the titration curve. pH-dependent properties of PLA-mPEG₂₀₀₀/TPGS₃₃₅₀-PHis-Folate nanoparticles may be caused by a lone pair electron on the unsaturated nitrogen in the imidazole ring of PHis segment [38, 39].

In vitro drug release

The in vitro release profiles of nanoparticles at pH 5.0, 6.5 and 7.4 are shown in Fig. 6. Within the first 10 h, the accumulated docetaxel release of the PLA–

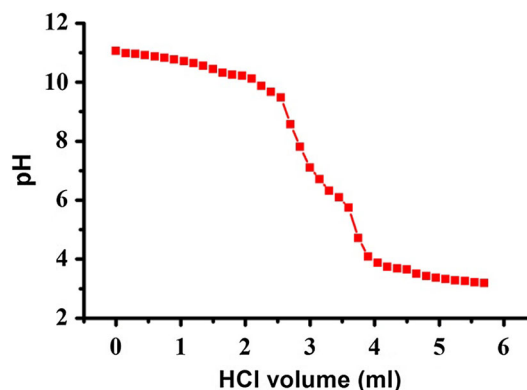


Figure 5 Acid–base titration profile of PLA-mPEG₂₀₀₀/TPGS₃₃₅₀-PHis-Folate nanoparticles with a weight ratio of 5:1.

mPEG₂₀₀₀/TPGS₃₃₅₀-PHis-Folate nanoparticles was 12% at pH 5.0, 10% at pH 6.5 and 2.7% at pH 7.4, respectively, which confirmed that PLA-mPEG₂₀₀₀/TPGS₃₃₅₀-PHis-Folate nanoparticles demonstrated pH-dependent drug release profiles, owing to pH-sensitive structure change of PHis in the nanoparticles.

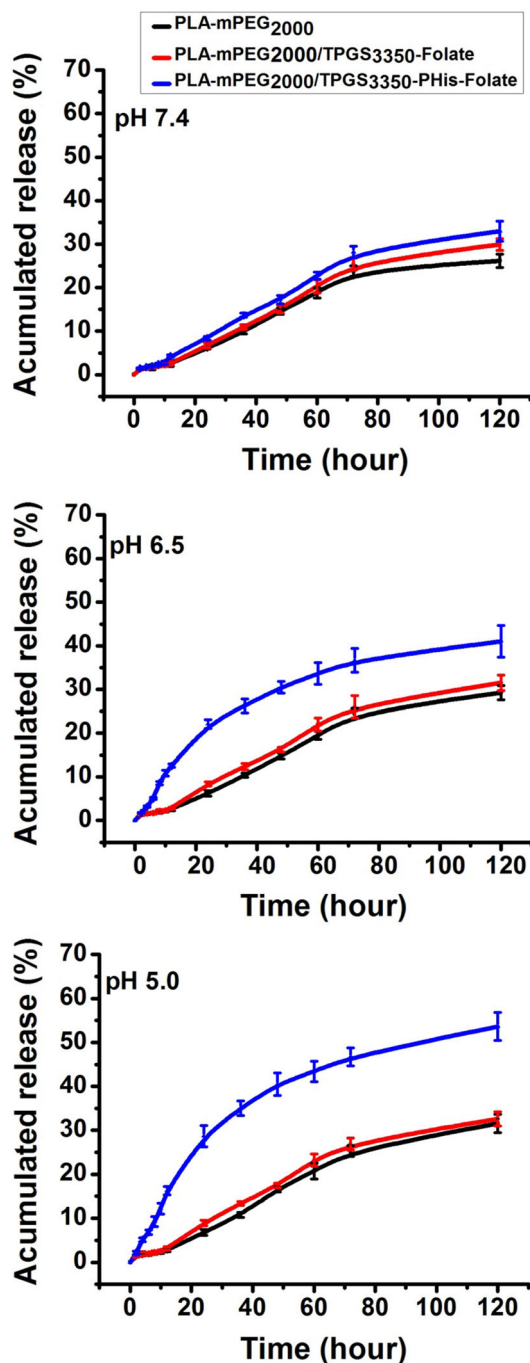


Figure 6 The release profiles of docetaxel from nanoparticles at different pH values.

As shown in Fig. 6, drug release from the PLA-mPEG₂₀₀₀/TPGS₃₃₅₀-PHis-Folate nanoparticles inside lysosomes (pH 5.0) within tumor cells is faster than that in the blood circulation environment (pH 7.4), achieving the objectives of fast intracellular drug delivery and enhanced antitumor effectivity of drug.

In vitro cellular uptake of nanoparticles

Figure 7 shows confocal laser scanning microscope (CLSM) images of 4T1 murine breast cancer cells after 4 h culture with the coumarin-6-loaded PLA-mPEG₂₀₀₀/TPGS₃₃₅₀-PHis-Folate nanoparticles suspension, at 0.1 mg/mL nanoparticles concentration at 37 °C at pH 7.4, 6.8, 5.8, respectively.

At pH 7.4, the slight intensity of green fluorescence from PLA-mPEG₂₀₀₀/TPGS₃₃₅₀-PHis-Folate nanoparticles in Fig. 7, which are similar to those of PLA-mPEG₂₀₀₀ nanoparticles and PLA-mPEG₂₀₀₀/TPGS₃₃₅₀-Folate nanoparticles without PHis-functionalization, in comparison with nanoparticles in Fig. 7b1 at pH 6.8 and Fig. 7c1 at pH 5.8, showed slow cellular uptake. These findings confirmed that PLA-mPEG₂₀₀₀/TPGS₃₃₅₀-PHis-Folate nanoparticles

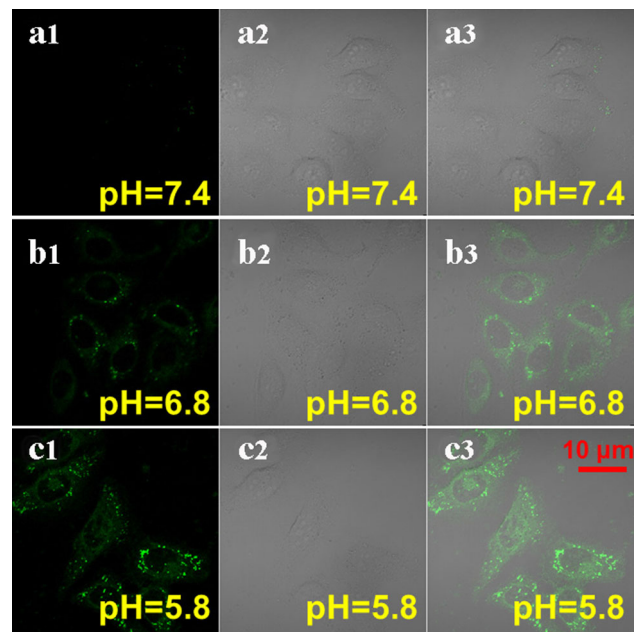


Figure 7 CLSM images of 4T1 murine breast cancer cells after 4 h culture with the coumarin-6-loaded PLA-mPEG₂₀₀₀/TPGS₃₃₅₀-PHis-Folate nanoparticles suspension at 0.1 mg/mL nanoparticles concentration at 37 °C at pH 7.4, 6.8, 5.8, respectively. (a1–a3: pH 7.4; b1–b3: pH 6.8; c1–c3: pH 5.8). The three photographs from left to right were coumarin-6, bright field and merged graphs.

exhibited higher and faster cellular uptake by 4T1 murine breast cancer cells than those with targeting or/and pH sensitive, which is helpful for enhancing the efficacy of chemotherapy.

In vitro cytotoxicity

It is evident in Fig. 8 that blank sample (no nanoparticles formulation) had almost no cytotoxicity to 4T1 murine breast cancer cells at pH 7.4, 6.8 and 5.8, suggesting the cytotoxicity of pH change can be neglected. The in vitro cytotoxicity of docetaxel-loaded PLA-mPEG₂₀₀₀ nanoparticles, PLA-mPEG₂₀₀₀/TPGS₃₃₅₀-Folate nanoparticles, PLA-mPEG₂₀₀₀/TPGS₃₃₅₀-PHis-Folate nanoparticles, at pH 7.4 (normal tissue), pH 6.8 (tumor extracellular space) and pH 5.8 (early endosomal compartment) were evaluated using CCK-8 assays. At pH 7.4, 6.8 and 5.8, PLA-mPEG₂₀₀₀/TPGS₃₃₅₀-PHis-Folate nanoparticles demonstrated significant advantages verse PLA-

mPEG₂₀₀₀ nanoparticles and PLA-mPEG₂₀₀₀/TPGS₃₃₅₀-Folate nanoparticles. For example, at pH 7.4, 4T1 murine breast cancer cells viability was decreased from 82.17% for PLA-mPEG₂₀₀₀ nanoparticles to 69.72% for the PLA-mPEG₂₀₀₀/TPGS₃₃₅₀-Folate nanoparticles, which is a 15.15% increase in cellular cytotoxicity; and 54.82% for PLA-mPEG₂₀₀₀/TPGS₃₃₅₀-PHis-Folate nanoparticles, which is a 33.28% increase in cellular cytotoxicity at the drug concentrations of 4 µg/mL after 8 h incubation.

Similar trends were also observed at the other drug concentrations and pH value. But PLA-mPEG₂₀₀₀/TPGS₃₃₅₀-PHis-Folate nanoparticles showed diverse cytotoxicity toward 4T1 murine breast cancer cells at different pH values. For instance, 4T1 murine breast cancer cells decreased in cell viability at 4 µg/mL drug concentrations after 8-h incubation from 54.82% at pH 7.4 to 33.07% at pH 6.8 and to 14.31% at pH 5.8, which is a 1.66-fold and 3.83-fold decrease, respectively. Perhaps, this is because that folate in PLA-mPEG₂₀₀₀/TPGS₃₃₅₀-PHis-Folate nanoparticles can bind folate receptors on cell membranes, triggering fast endocytosis into lysosomes, followed by rapid intracellular drug release. Therefore, the results indicated that the pH-sensitive PLA-mPEG₂₀₀₀/TPGS₃₃₅₀-PHis-Folate nanoparticles demonstrated significantly increased in vitro therapeutic effects.

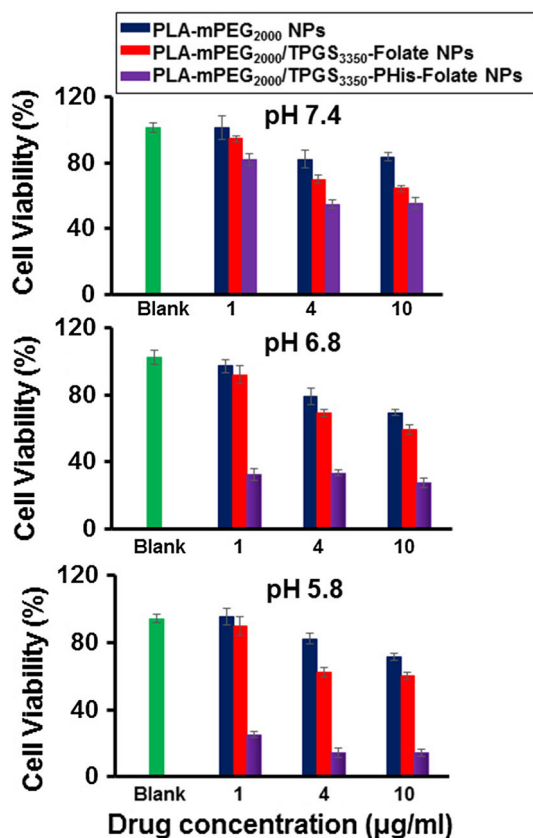


Figure 8 In vitro cell viability of 4T1 murine breast cancer cells with various nanoparticles formulations at 1, 4, 10 µg/mL drug concentration, after 8 h incubation at pH 7.4, 6.8, 5.8, respectively.

Conclusions

In this study, a novel pH-sensitive copolymer of TPGS₃₃₅₀-PHis-Folate was synthesized. The nanoparticles containing pH-sensitive TPGS₃₃₅₀-PHis-Folate and PLA-mPEG₂₀₀₀ were prepared by the nanoprecipitation method with docetaxel as a model anticancer drug. The PLA-mPEG₂₀₀₀/TPGS₃₃₅₀-PHis-Folate nanoparticles combined active targeting with pH-triggered quick drug release could achieve fast cellular uptake of the nanoparticles and enhanced accumulation in tumor tissues for the better therapeutic efficacy of drug-loaded nanoparticles systems. Thus, the drug-loaded PLA-mPEG₂₀₀₀/TPGS₃₃₅₀-PHis-Folate nanoparticles designed in this work have great potential to be used for chemotherapy.

Acknowledgements

This research work was financially supported by the National Natural Science Foundation of China (No. 21506161, 21646010 and 21476172) and Open Funds from the key laboratory of biomedical materials in Tianjin (No. 1634-1).

Compliance with ethical standards

Conflict of interest The authors declare that they have no conflict of interest.

References

- [1] Siegel RL, Miller KD, Jemal A (2016) Cancer statistics, 2016. *CA Cancer J Clin* 66(1):7–30
- [2] Schiller JH, Harrington D, Belani CP, Langer C, Sandler A, Krook J, Zhu JM, Johnson DH, Eastern G (2002) Cooperative oncology, comparison of four chemotherapy regimens for advanced non-small-cell lung cancer. *N Engl J Med* 346(2):92–98
- [3] Zitvogel L, Apetoh L, Ghiringhelli F, Kroemer G (2008) Immunological aspects of cancer chemotherapy. *Nat Rev Immunol* 8(1):59–73
- [4] Pelaz B, Alexiou C, Alvarez-Puebla RA, Alves F, Andrews AM, Ashraf S, Balogh LP, Ballerini L, Bestetti A, Brendel C (2017) Diverse applications of nanomedicine. *ACS Nano* 11(3):2313–2381
- [5] Sun T, Zhang YS, Pang B, Hyun DC, Yang M, Xia Y (2014) Engineered nanoparticles for drug delivery in cancer therapy. *Angew Chem Int Ed* 53(46):12320–12364
- [6] Blanco E, Shen H, Ferrari M (2015) Principles of nanoparticle design for overcoming biological barriers to drug delivery. *Nat Biotechnol* 33(9):941–951
- [7] Kamaly N, Yameen B, Wu J, Farokhzad OC (2016) Degradable controlled-release polymers and polymeric nanoparticles: mechanisms of controlling drug release. *Chem Rev* 116(4):2602–2663
- [8] Nicolas J, Mura S, Brambilla D, Mackiewicz N, Couvreur P (2013) Design, functionalization strategies and biomedical applications of targeted biodegradable/biocompatible polymer-based nanocarriers for drug delivery. *Chem Soc Rev* 42(3):1147–1235
- [9] Ulbrich K, Hola K, Subr V, Bakandritsos A, Tucek J, Zboril R (2016) Targeted drug delivery with polymers and magnetic nanoparticles: covalent and noncovalent approaches, release control, and clinical studies. *Chem Rev* 116(9):5338–5431
- [10] Dai Y, Xu C, Sun X, Chen X (2017) Nanoparticle design strategies for enhanced anticancer therapy by exploiting the tumour microenvironment. *Chem Soc Rev* 46(12):3830–3852
- [11] Stewart MP, Sharei A, Ding X, Sahay G, Langer R, Jensen KF (2016) In vitro and ex vivo strategies for intracellular delivery. *Nature* 538(7624):183–192
- [12] Bourzac K (2016) Cancer nanomedicine, reengineered After recent setbacks, researchers hope to find approaches more attuned to the complexities of cancer biology. *Proc Natl Acad Sci USA* 113(45):12600–12603
- [13] Shi J, Kantoff PW, Wooster R, Farokhzad OC (2017) Cancer nanomedicine: progress, challenges and opportunities. *Nat Rev Cancer* 17(1):20–37
- [14] Pozzi D, Colapicchioni V, Caracciolo G, Piovesana S, Capriotti AL, Palchetti S, De Grossi S, Riccioli A, Amenitsch H, Lagana A (2014) Effect of polyethyleneglycol (PEG) chain length on the bio-nano-interactions between PEGylated lipid nanoparticles and biological fluids: from nanostructure to uptake in cancer cells. *Nanoscale* 6(5):2782–2792
- [15] Du J, Lane LA, Nie S (2015) Stimuli-responsive nanoparticles for targeting the tumor microenvironment. *J Control Release* 219:205–214
- [16] Karimi M, Ghasemi A, Zangabad PS, Rahighi R, Basri SMM, Mirshekari H, Amiri M, Pishabad ZS, Aslani A, Bozorgomid M, Ghosh D, Beyzavi A, Vaseghi A, Aref AR, Haghani L, Bahrami S, Hamblin MR (2016) Smart micro/nanoparticles in stimulus-responsive drug/gene delivery systems. *Chem Soc Rev* 45(5):1457–1501
- [17] Mura S, Nicolas J, Couvreur P (2013) Stimuli-responsive nanocarriers for drug delivery. *Nat Mater* 12(11):991–1003
- [18] Hu J, Miura S, Na K, Bae YH (2013) pH-responsive and charge shielded cationic micelle of poly(L-histidine)-block-short branched PEI for acidic cancer treatment. *J Control Release* 172(1):69–76
- [19] Lee ES, Na K, Bae YH (2005) Super pH-sensitive multifunctional polymeric micelle. *Nano Lett* 5(2):325–329
- [20] Zhou Z, Badkas A, Stevenson M, Lee JY, Leung YK (2015) Herceptin conjugated PLGA-PHis-PEG pH sensitive nanoparticles for targeted and controlled drug delivery. *Int J Pharm* 487(1):81–90
- [21] Ko H, Son S, Jeon J, Thambi T, Kwon S, Chae YS, Young MK, Park JH (2016) Tumor microenvironment-specific nanoparticles activatable by stepwise transformation. *J Control Release* 234:68–78
- [22] Yang KN, Zhang CQ, Wang W, Wang PC, Zhou JP, Liang XJ (2014) pH-responsive mesoporous silica nanoparticles employed in controlled drug delivery systems for cancer treatment. *Cancer Biol Med* 11(1):34–43
- [23] Lu Y, Aimetti AA, Langer R, Gu Z (2016) Bioresponsive materials. *Nat Rev Mater* 2 16075:1–17

- [24] Alvarez-Lorenzo C, Concheiro A (2014) Smart drug delivery systems: from fundamentals to the clinic. *Chem Commun* 50(58):7743–7765
- [25] Lee ES, Gao Z, Bae YH (2008) Recent progress in tumor pH targeting nanotechnology. *J Control Release* 132(3):164–170
- [26] Li Z, Qiu L, Chen Q, Hao T, Qiao M, Zhao H, Zhang J, Hu H, Zhao X, Chen D, Mei L (2015) pH-sensitive nanoparticles of poly(L-histidine)-poly(lactide-co-glycolide)-tocopheryl polyethylene glycol succinate for anti-tumor drug delivery. *Acta Biomater* 11:137–150
- [27] Wu H, Zhu L, Torchilin VP (2013) pH-sensitive poly(histidine)-PEG/DSPE-PEG co-polymer micelles for cytosolic drug delivery. *Biomaterials* 34(4):1213–1222
- [28] Liu R, Li D, He B, Xu X, Sheng M, Lai Y, Wang G, Gu Z (2011) Anti-tumor drug delivery of pH-sensitive poly(ethylene glycol)-poly(L-histidine)-poly(L-lactide) nanoparticles. *J Control Release* 152(1):49–56
- [29] Pan J, Feng SS (2008) Targeted delivery of paclitaxel using folate-decorated poly(lactide)-vitamin E TPGS nanoparticles. *Biomaterials* 29(17):2663–2672
- [30] Mi Y, Liu Y, Feng SS (2011) Formulation of docetaxel by folic acid-conjugated α -tocopheryl polyethylene glycol succinate 2000 (vitamin E TPGS) micelles for targeted and synergistic chemotherapy. *Biomaterials* 32(16):4058–4066
- [31] Zhang Z, Mei L, Feng SS (2012) Vitamin E D- α -tocopheryl polyethylene glycol 1000 succinate-based nanomedicine. *Nanomedicine* 7(11):1645–1647
- [32] Pan J, Wan D, Bian Y, Guo Y, Jin F, Wang T, Gong J (2014) Reduction of nonspecific binding for cellular imaging using quantum dots conjugated with vitamin E. *Aiche J* 60(5):1591–1597
- [33] Lee ES, Shin HJ, Na K, Bae YH (2003) Poly(L-histidine)-PEG block copolymer micelles and pH-induced destabilization. *J Control Release* 90(3):363–374
- [34] Liu R, He B, Li D, Lai Y, Tang JZ, Gu Z (2012) Synthesis and characterization of poly(ethylene glycol)-b-poly(L-histidine)-b-poly(L-lactide) with pH-sensitivity. *Polymer* 53(7):1473–1482
- [35] Pan J, Liu Y, Feng SS (2010) Multifunctional nanoparticles of biodegradable copolymer blend for cancer diagnosis and treatment. *Nanomedicine* 5(3):347–360
- [36] Philipsen HJA (2004) Determination of chemical composition distributions in synthetic polymers. *J Chromatogr A* 1037(1):329–350
- [37] Pan J, Wang Y, Feng SS (2008) Formulation, characterization, and in vitro evaluation of quantum dots loaded in poly(lactide)-vitamin E TPGS nanoparticles for cellular and molecular imaging. *Biotechnol Bioeng* 101(3):622–633
- [38] Radovic-Moreno AF, Lu TK, Puscasu VA, Yoon CJ, Langer R, Farokhzad OC (2012) Surface charge-switching polymeric nanoparticles for bacterial cell wall-targeted delivery of antibiotics. *ACS Nano* 6(5):4279–4287
- [39] Lee ES, Oh KT, Kim D, Youn YS, Bae YH (2007) Tumor pH-responsive flower-like micelles of poly(L-lactic acid)-b-poly(ethylene glycol)-b-poly(L-histidine). *J Control Release* 123(1):19–26